IIETA International Information and Engineering Technology Association
Advancing the World of Information and Engineering

Annales de Chimie - Science des Matériaux
Vol. 48, No. 1, February, 2024, pp. 73-83
Journal homepage: http://iieta.org/journals/acsm

Synthesis, Characterization, and Infrared Blocking Efficiency of Polyvinyl Alcohol Composites Filled with Cadmium Sulfide and Zinc Sulfide NPs

Zainab Hasan Ali*, Ali S. Hasan, Auda Jabbar Braihi

Department of Polymer and Petrochemical Industries, College of Materials Engineering, University of Babylon, Babylon 51001, Iraq

Corresponding Author Email: zainab.ali.math89@student.uobabylon.edu.iq

https://doi.org/10.18280/acsm.480109

Received: 30 September 2023
Revised: 28 November 2023
Accepted: 1 January 2024
Available online: 26 February 2024

Keywords:
nano composite, semiconductors sustainability applications, infrared blocking, PVA-ZnS, PVA-CdS, sol-gel method, heat transfer

ABSTRACT

This investigation explores the efficiency of composite coatings, leveraging polyvinyl alcohol (PVA) matrices embedded with zinc sulfide (ZnS) and cadmium sulfide (CdS) nanoparticles, for their infrared (IR) radiation blocking potential. Such coatings are strategically synthesized via a sol-gel method, targeting applications that demand IR attenuation, including but not limited to, construction, architectural fenestrations, vehicular glazing, and thermal insulation domains. In these composites, meticulous integration of ZnS and CdS nanoparticles within the PVA framework was demonstrated to significantly bolster their IR reflective or absorptive properties, consequently curtailing heat transference. It has been observed that nanoparticle concentration and coating thickness serve as critical factors, directly correlating with the IR-blocking proficiency—enhanced concentrations and augmented thicknesses invariably yield superior performance metrics. The surface morphology, assessed through Atomic Force Microscopy (AFM), revealed a positive correlation between nanoparticle concentration and surface roughness, paralleling an increase in particle size. This observation is corroborated by scanning electron microscopy, attesting to the uniform nanoparticle distribution. Fourier-transform infrared spectroscopy (FTIR) analysis identified novel peaks at approximately 1280 and 1700 cm^{-1}, indicative of a chemical interaction between ZnS nanoparticles and the PVA matrix, as evidenced by the presence of reactive functional groups on the ZnS nanoparticle surface. Thermogravimetric analysis (TGA) imparted insights into the thermal stability of the specimens, with CdS composites exhibiting a weight loss of 98.73%, in stark contrast to the 91.04% manifested by the ZnS counterparts. The disparity is attributed to the higher boiling point of CdS (1750℃) vis-à-vis ZnS (1700℃), underscoring the material's intrinsic thermal resilience. The findings from this research underscore the potential of PVA-ZnS and PVA-CdS coatings as viable candidates for IR-blocking applications, positing an innovative solution to thermal management challenges in various sectors.

1. INTRODUCTION

Infrared (IR) radiation-blocking coatings are at the forefront of technological advances across aerospace, defense, and energy industries, providing enhanced thermal insulation, concealment capabilities, and energy efficiency [1, 2]. The pursuit of effective IR-blocking materials has led researchers to explore a myriad of compositions, with polyvinyl alcohol (PVA), cadmium sulfide (CdS), and zinc sulfide (ZnS) emerging as materials of considerable interest [3, 4].

Polyvinyl alcohol is noted for its film-forming prowess, biocompatibility, and processing versatility, which have been exploited in coatings, adhesives, and packaging [5]. Meanwhile, CdS and ZnS—semiconductors with wide bandgaps—are distinguished by optical properties that align well with IR-blocking applications; they exhibit high transparency in the visible spectrum, along with potent IR absorption and reflection [6-10].

The integration of CdS or ZnS nanoparticles (NPs) into a PVA matrix yields composite coatings with enhanced IR-blocking capabilities [11]. This synergy leverages the film-forming strengths of PVA with the optical advantages of the semiconductor materials, culminating in coatings with superior IR-blocking properties [12]. These composites have been the subject of extensive research, focusing on their potential for diverse applications [13-15].

Such coatings also offer the benefits of flexibility, durability, and ease of application. The PVA matrix serves to stabilize mechanically and shield the semiconductor NPs, thereby extending the lifespan of the coatings [16-18]. The binder properties of PVA facilitate the coating process on various substrates, including metals, plastics, and textiles.

The application scope for PVA/CdS and PVA/ZnS composites is vast. In aerospace, the coatings are pivotal for the advancement of stealth technologies, minimizing the IR signature of aircraft and drones [19, 20]. The defense sector can utilize these coatings for camouflage, enhancing the concealment of personnel and equipment in combat [21, 22].

For the energy sector, the application of these coatings in buildings promises substantial improvements in thermal insulation, leading to energy conservation and reduced climate control expenses [1, 23, 24].

It is crucial to characterize composites such as PVA/ZnS and PVA/CdS for their optical properties to harness their full potential in optical devices. Analyzing their absorbance, emission, and transparency is imperative to refine their functionalities in sensors, photovoltaic cells, light-emitting diodes, and other optical instruments. This research aims to bridge knowledge gaps by presenting a detailed examination of the optical behavior of PVA/ZnS and PVA/CdS composites, particularly in response to variations in composite ratios, synthesis methodologies, and environmental conditions.

The current study is dedicated to the preparation and characterization of polymeric composites doped with ZnS or CdS for optical applications, with an aim to optimize electrical energy consumption. The investigation encompasses structural, optical, morphological, and electrical properties of the fabricated films.

It has been established that nanoparticle concentration and coating thickness are critical determinants of IR-blocking efficiency in PVA/ZnS and PVA/CdS coatings [11-15]. An increase in either parameter typically results in a more pronounced IR-blocking effect, attributed to the heightened probability of incident IR radiation encountering and being absorbed by the nanoparticles. The presence of additional layers and a higher density of particles introduce more obstacles to the passage of IR radiation, thus enhancing the coatings' ability to impede IR wavelengths.

2. EXPERIMENTAL PART

2.1 Synthesis of PVA/NPs (CdS or ZnS) thin films

(1). Dissolve PVA powder] with different weight fraction (demonstrate Tables 1 and 2) in 100ml of distilled water to create a PVA solution.
(2). Disperse NPs (CdS or ZnS) NPs in a suitable solvent, such as ethanol or water. It has been dissolved in 100ml of distilled water. This step aims to achieve a homogeneous mixture of NPs in the liquid phase.
(3). Combine the PVA solution and NPs (ZnS or CdS) dispersion in the desired ratio (demonstrate Table 2).
(4). Agitate the mixture to ensure thorough mixing and dispersion of the NPs within the PVA solution. Stirring with a magnetic stirrer (2 hours) or sonication can be used for this purpose (30 min).
Apply the PVA-NPs mixture onto the desired substrate using (5). A suitable thin film coating method. Some commonly used methods include spin coating, dip coating, spray coating, or doctor blade coating. The choice of method depends on factors such as the substrate material, film thickness requirements, and equipment availability. It has been used dip coating and casting methods (Depending on the shape of the specimen required for examination). The concentration of NPs and the thickness of the coating in a composite material can significantly impact its IR-blocking efficiency. Higher nanoparticle concentrations or thicker coatings generally enhance IR-blocking efficiency due to increased absorption and scattering of infrared radiation. The greater the concentration or thicker the coating, the more material is available to interact with and block the infrared wavelengths, thereby improving the overall blocking capability of the composite. However, there might be an optimal range or threshold beyond which further increases in concentration or thickness might not significantly enhance IR-blocking efficiency and could lead to diminishing returns or changes in other material properties. The specifics depend on the type of NPs, their properties, and the composite material's characteristics.
(6). Allow the coated substrate to dry in a controlled environment. This step involves removing the solvent from the coating, typically by evaporation. Depending on the solvent used, drying can be achieved by using an oven for 7 hours at 80°C. Curing may also be necessary to enhance the film's properties, which can be done by subjecting the film to heat or other appropriate treatments.

Table 1. The specifications of the primary materials

Name	Poly (Vinyl Alcohol) (PVA)	Cadmium Sulfide (CdS)	Zinc Sulfide (ZnS)
Molecular formula	[-CH2CHOH-]n	CdS	ZnS
Molecular weight (g/mol)	1,60,000	144.46	97.474
Color	White	Yellow	White
Shape	Powder	NPs	NPs
Supplier	Nashik , india	China	British

Table 2. The added weight percent of NPs to PVC

PVA (wt%)	NPs (wt%) (CdS or ZnS)
100	0
96	4
88	12
84	16

3. RESULTS AND DISCUSSIONS

3.1. Optical result

The thin film coating of PVA/NPs exhibits low transmission and a low energy gap with increases concentration of NPs (ZnS or CdS), it means that it is effective in blocking infrared (IR) radiation as demonstrated in Figures 1 and 2. The low transmission indicates that the film does not allow much IR light to pass through, while the low energy gap implies that the film has a narrow range of energy levels where it absorbs IR radiation. This combination makes the thin film coating suitable for IR-blocking coating.

When IR radiation interacts with the thin film coating, it can be absorbed by the film material. The absorption occurs when the energy of the IR photons matches the energy levels within the low energy gap of the film. As a result, the film converts the absorbed energy into heat, preventing it from passing through the coating. The absorbed IR radiation is effectively "trapped" within the film, reducing its transmission through the coating.

In addition to absorption, the thin film coating can also reflect a portion of the incident IR radiation. As demonstrated in in subgraph (a) of Figure 1, where it has been noticed that the absorbance continues to stabilize with increasing wavelength, but this absorbance of the specimens under study (PVA-ZnS) increases with the increase in the addition percentage of (ZnS) compound slightly These are consistent with the results of researchers [17, 19].

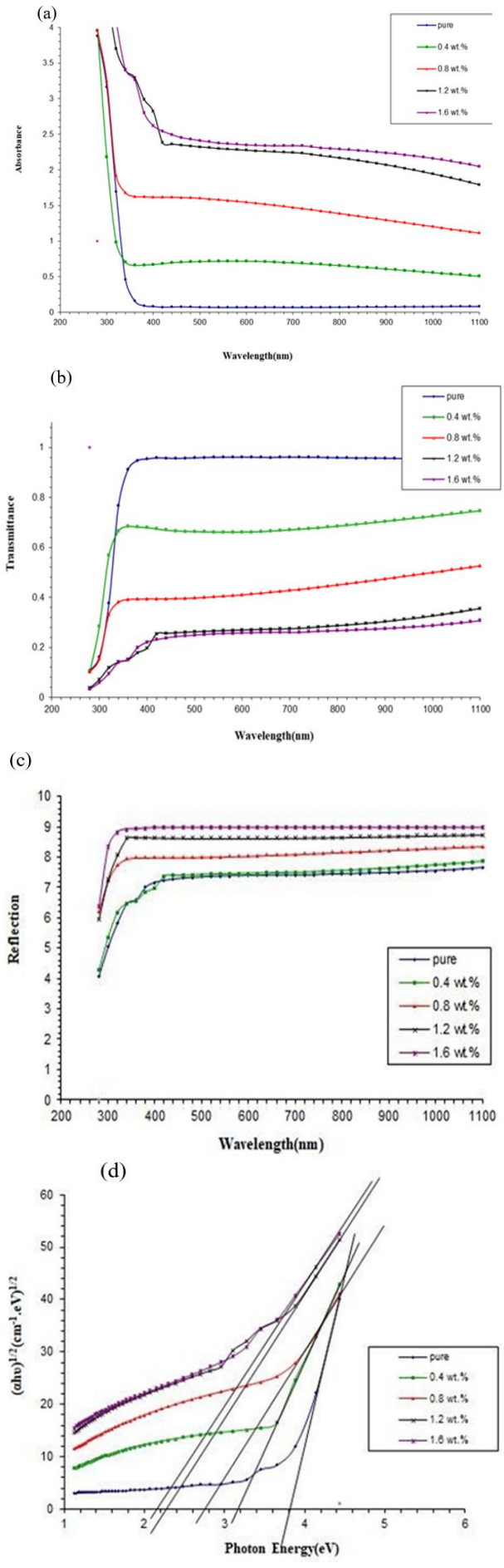

Figure 1. Optical properties of PVA/ZnS (a) absorption (b) transmission (c) Reflection (d) energy band

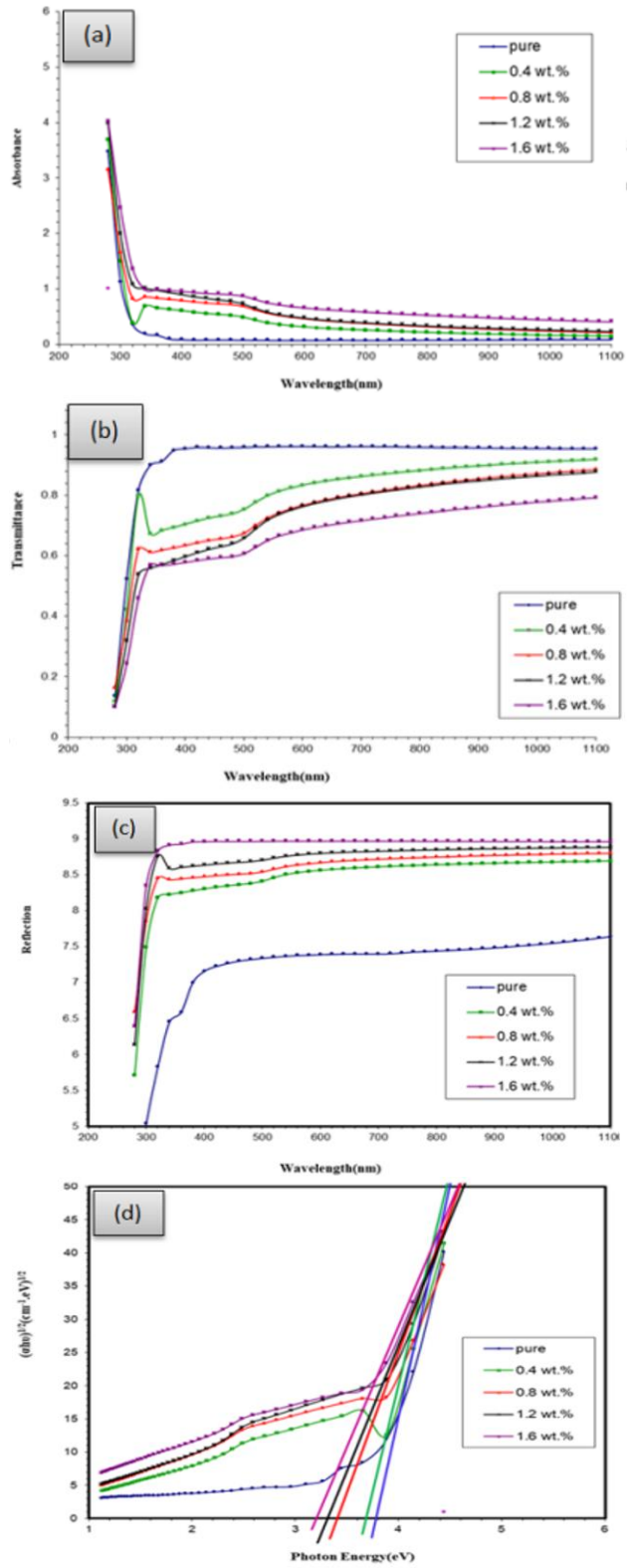

Figure 2. Optical properties of PVA/CdS (a) Absorption (b) Transmission (c) Reflection (d) Energy band

This behavior is like the absorbance behavior of the (PVA-CdS) films, where the absorbance also increases with the increase in the concentration of a compound (CdS). As demonstrated in subgraph (a) of Figure 2, this is since the increase of the number of charge carriers with increasing content of NPs.

This behavior is useful for optoelectronics, photocatalysis and solar cells. In a broad sense, it can be identified that the absorbance of all the prepared nanocomposites exhibits a

decrease as the wavelength increases. In the realm of materials engineering, this signifies that the electron within the nanocomposites remains unexcited by the incident photon since the photon's energy being insufficient to bridge the energy gap between the electron's lower energy level and the desired higher energy level.

While Figures 1b and 2b demonstrate the transmittance spectrum of the prepared films, as the transmittance decreases with increasing concentration, and this confirms the validity of the results. With increasing absorbance, the transmittance decreases, albeit slightly according to the law of conservation of energy. this is since the agglomeration of NPs with increasing content and increase of the number of charge carriers These are consistent with the results of researchers [21, 25].

The reflection occurs when the energy of the IR photons does not match the energy levels within the low energy gap, causing them to bounce off the surface of the coating. The reflected IR radiation is redirected away from the coated material, further reducing its penetration.

Through Figures 1c and 2c, it has been noticed that the reflectivity spectrum increases with the increase in the concentration ratio of (ZnS) and (CdS) compounds, and the reflectivity stabilizes from a wavelength of about (400 nm) and up to the infrared region of about (1100 nm), and this is important in terms of application for the uses of infrared reflection.

By combining absorption and reflection, the thin film coating effectively blocks the transmission of IR radiation. The absorbed energy is dissipated as heat within the film, and the reflected energy is redirected away from the coated surface. As a result, the IR radiation is prevented from passing through the coating and reaching the underlying materials or environment.

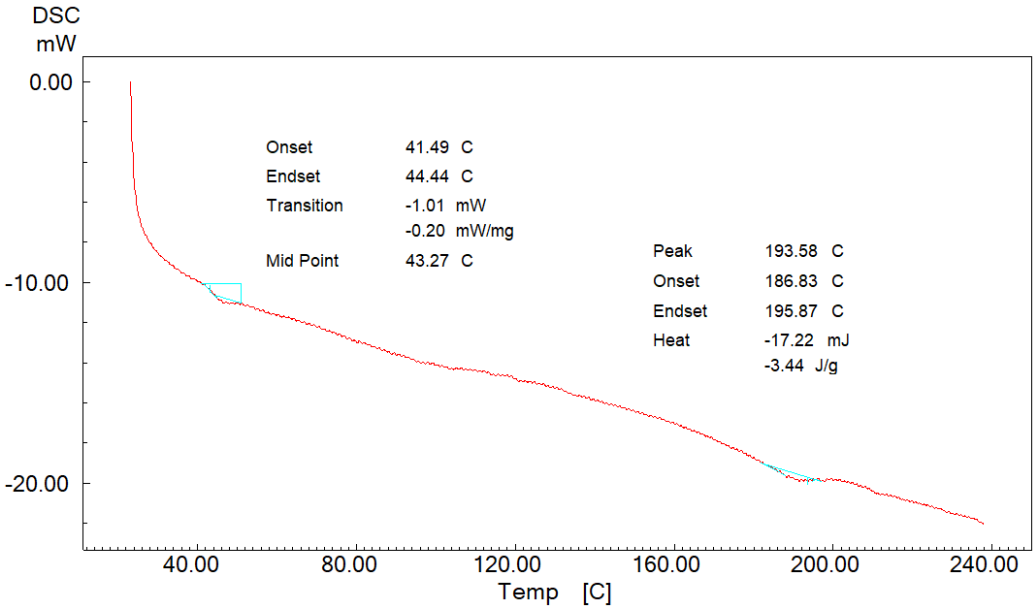

Figure 3. DSC curve of PVA/ 1.6 (wt%) ZnS NPs

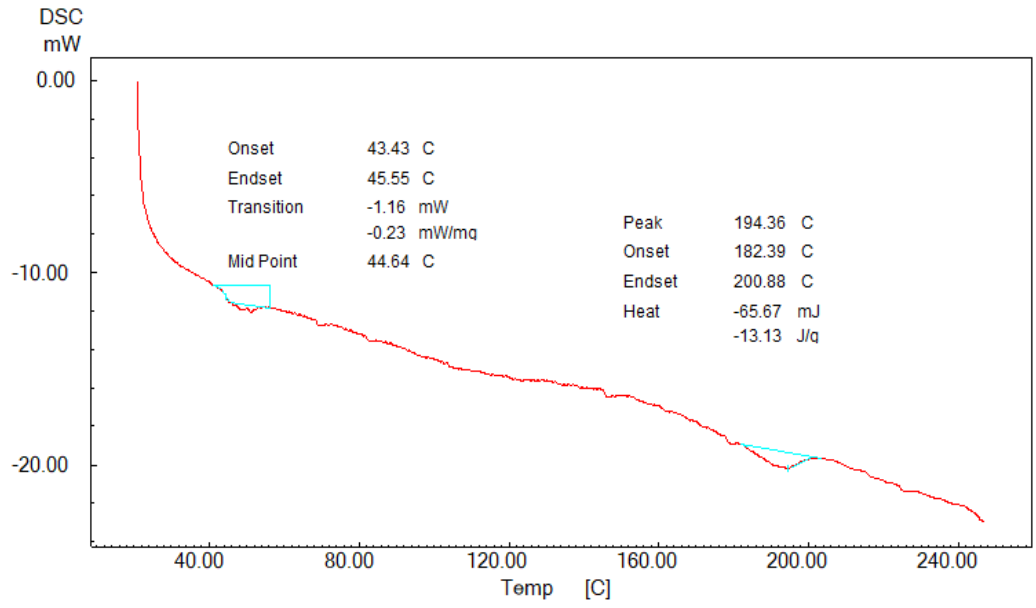

Figure 4. DSC curve of PVA/ 1.6 (wt%) ZnS NPs

Table 3. Thermal transitions of PVA/ ZnS NPs and PVA/CdS NPs

Filler Type	Glass Transition		Melting Transition	
ZnS NPs	Onset (oC)	41.49	Onset (oC)	180.83
	Endset (oC)	44.44	Endset (oC)	195.67
	Mid point (oC)	43.27	Peak (oC)	193.58
	Transition (mW/mg)	-0.2	Enthalpy (J/g)	-3.44
CdS NPs	Onset (oC)	43.43	Onset (oC)	182.39
	Endset (oC)	45.55	Endset (oC)	200.88
	Mid point (oC)	44.64	Peak (oC)	194.36
	Transition (mW/mg)	-0.23	Enthalpy (J/g)	-13.13

Figures 1d and 2d demonstrate the calculated energy gap, which demonstrated that the prepared films have a large gap value, and when CdS or ZnS materials were added, the value of that gap decreased, and this is since the generation of secondary levels of compounds added within the energy gap, which narrowed the gap and thus increased optical conductivity which is inversely proportional to the value of the energy gap, these are consistent with the results of researchers [10, 18, 26].

3.2 DSC results

Figures 3 and 4 demonstrate the DSC thermograms for the highest percentage of PVA/ ZnS NPs and PVA/CdS NPs respectively. In both curves, there are two endothermic transitions: glass and melting. CdS semiconductor NPs increase both the above transitions, where the Tg increased from 43.27 to 44.64℃, the Tm increased from 193.58 to 194.36℃ and the enthalpy increased from -3.44 to -13.13 J/g as shown in (Table 3). Many reasons stand behind these behaviors, such as the type of chemical functional groups, surface morphologies and so on. These are consistent with the results of researchers [21, 25, 27].

3.3 FTIR result

Figure 5 demonstrates the FTIR characteristics bands for pure PVA, where there is some overlapping between C-H stretching and C-C stretching along wavenumbers from 2600-3400 cm-1. The band at 1650.78 cm-1 for C=O stretching and bands from 1371.35 to 1417.32 cm-1 are for C-H bending. Band at 1082.46 cm-1 for C-O stretching, the band at 914.33 cm-1 for CH2 rocking and the band at 835 cm-1 for C-C stretching. These are consistent with the results of researchers [7, 24].

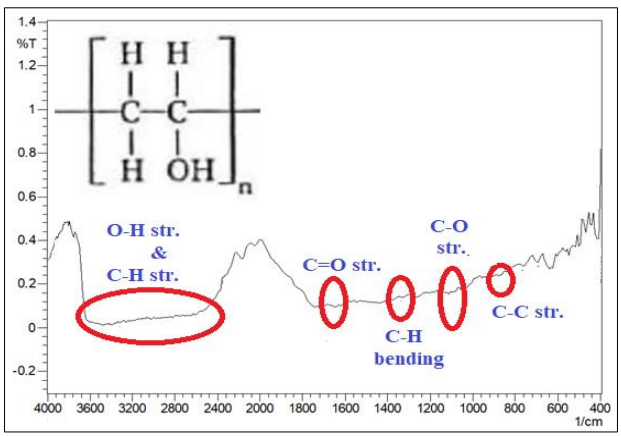

Figure 5. FTIR spectrum of pure PVA

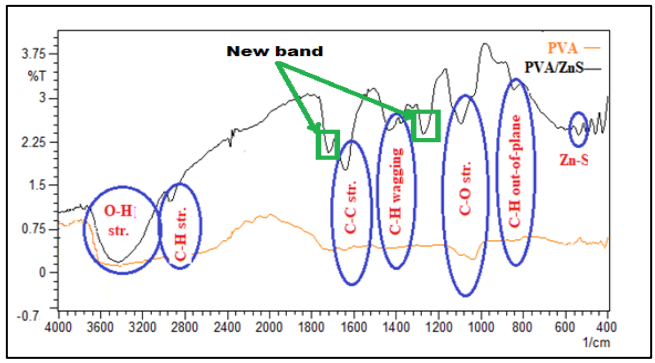

Figure 6. FTIR spectra of pure PVA and PVA/ 1.4 wt% ZnS

The presence of new pulses at about 1280 and 1700 cm^{-1} as shown in (Figure 6) confirms the occurrence of a chemical reaction between ZnS NPs and PVA since the availability of many active functional groups on the surface of ZnS NP. Indeed, often NP surfaces are very reactive and have many active cites and high surface area to volume ratio.

The FTIR spectrum PVA/CdS NPs (Figure 3) revealed bands at 1040, 1116, 1645, 2923 and 3438, cm^{-1} which correspond to stretching of C–N, sulfide compounds, amide I bands of proteins and hydrogen bonding respectively.

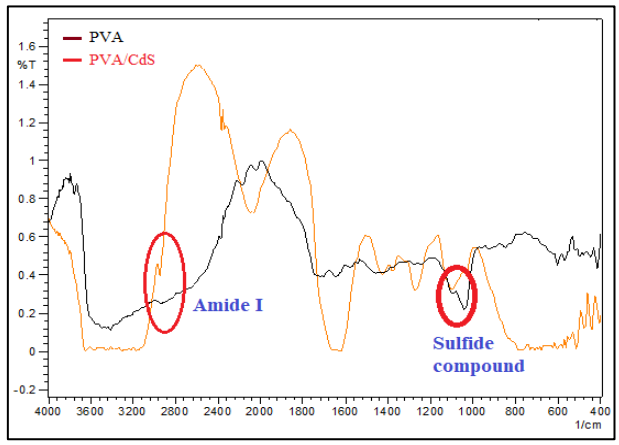

Figure 7. FTIR spectra of pure PVA and PVA/ 1.4 wt% CdS

After CdS NPs addition, the intensities of most groups were increased compared with those of pure PVA (Figure 7). This is since the similarities of the chemical groups in the PVA polymer and those available on the CdS NPs [13].

3.4 TGA result

Figures 8 and 9 demonstrate the TGA curves of PVA/ 1.6 wt% CdS and PVA/ 1.6 wt% ZnS respectively. Up to 900℃, the weight loss of the CdS specimen is 98.73%, while for ZnS

specimen it is only 91.04%. This is because that CdS have higher boiling point (1750oC) than ZnS (1700oC) [14, 15].

The specimen containing CdS loses its weight in two stages, where the first one ended at about 150 oC, while the second stage extended up to 900 oC and experiencing a gradual loss. In the first stage, there is a loss of water and light volatile compounds, while during the second stage there is a thermal decomposition of the PVA polymer. These are consistent with the results of researchers [6, 22, 28].

The specimen containing ZnS loses its weight upon three stages. In the first stage loses only about 2% in wide temperature range extended up to 300, which refers to high stability at the practice range. In this stage there is no significant mass change, thus considered as a plateau stage. In contrast, most weight loss occurred at the second stage, which extends up to 450, while there is a gradual loss in the third stage.

The overall findings from this test are:

1. All these composites can be used safely in the temperature range from room temperature up to 70oC.
2. These composites have long Lifetime.
3. These composites have a high ability to resist atmospheric oxidation.

Reasons for CdS having a higher weight loss:

1. Lower thermal stability: CdS typically exhibits lower thermal stability compared to ZnS. Hence, it may start decomposing or volatilizing at relatively lower temperatures.
2. Chemical composition: The chemical structure and composition of CdS might make it more prone to decomposition or vaporization at the TGA test temperatures compared to ZnS.

3.5 AFM results

Figures 10 and 11 display the topographic structures in 2D and 3D views of PVA/ZnS coated specimens with different ratios (4% and 16% respectively). These figures demonstrate that coated specimens are more homogeneous than pure PVA as shown in (Figure 12). The addition of NPs increases surface roughness and average diameter. These are consistent with the results of researchers [16, 21]. Figures 13 and 14 display the topographic structures in 2D and 3D views of PVA/CdS coated specimens with different ratios (4 and 16 wt% respectively). These figures demonstrate that coated specimens are more homogeneous than pure PVA. the addition of NPs increases surface roughness and average diameter, the reason may return to NPs to the PVA matrix might increase the roughness since the presence of larger particles or uneven distribution or agglomeration of NPs. This effect could be more pronounced with higher concentrations of NPs.

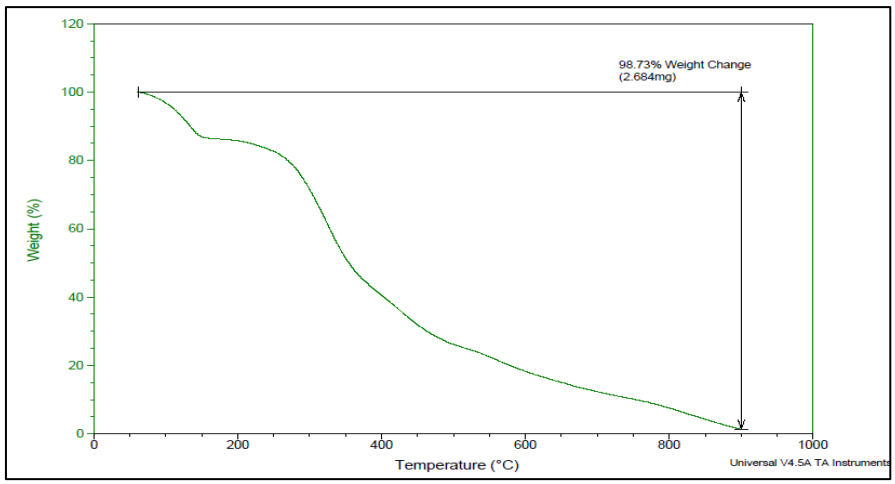

Figure 8. TGA curve for PVA/ 1.6 wt% Cds composite

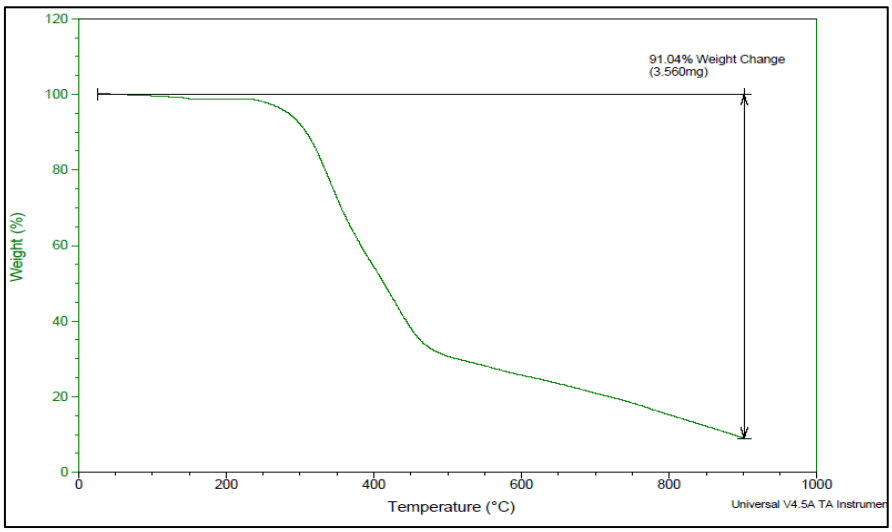

Figure 9. TGA curve for PVA/ 1.6 wt% ZnS composite

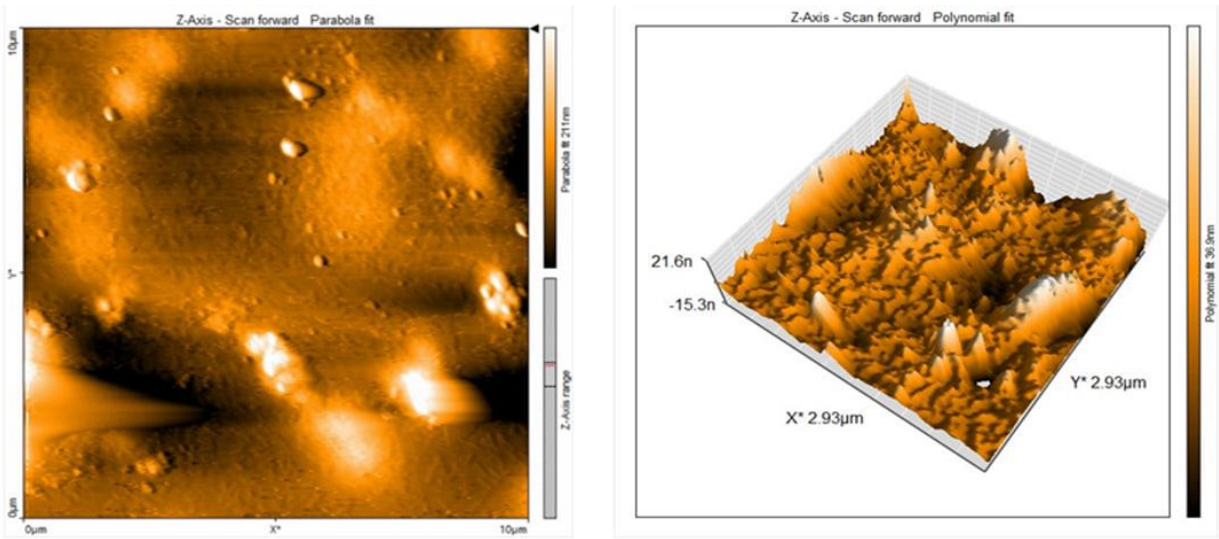

Figure 10. 2D and 3D AFM images of 4 wt% ZnS/ PVA)

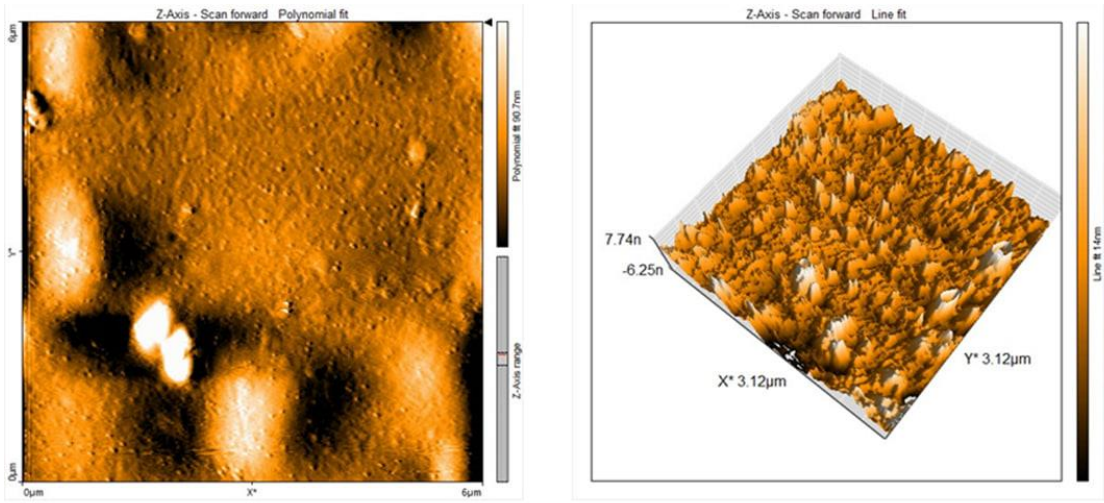

Figure 11. 2D and 3D AFM images of 16 wt% ZnS / PVA)

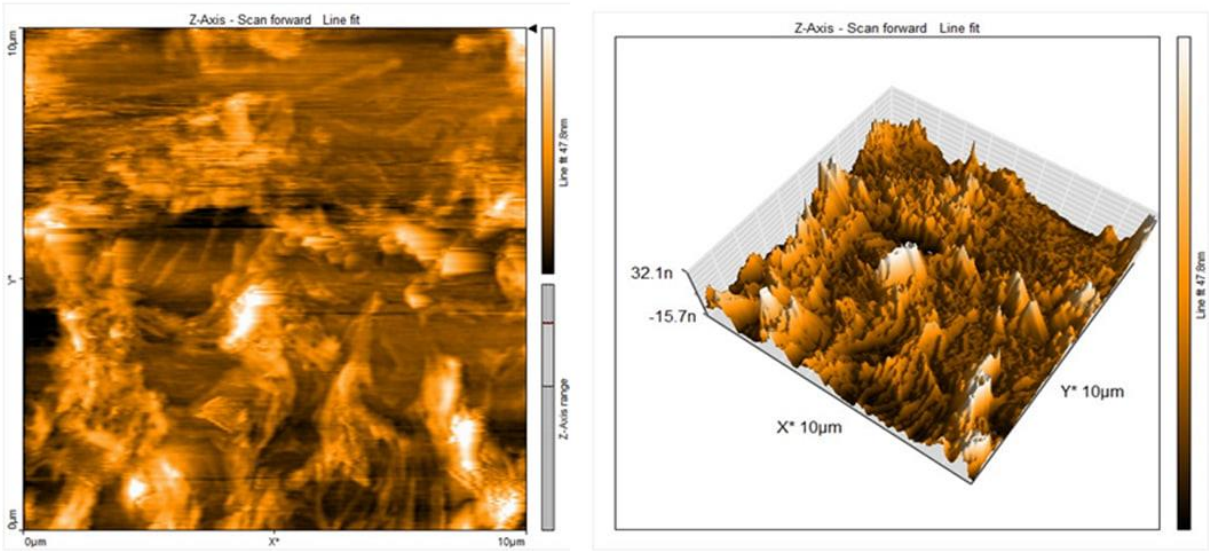

Figure 12. 2D and 3D AFM images of pure PVA

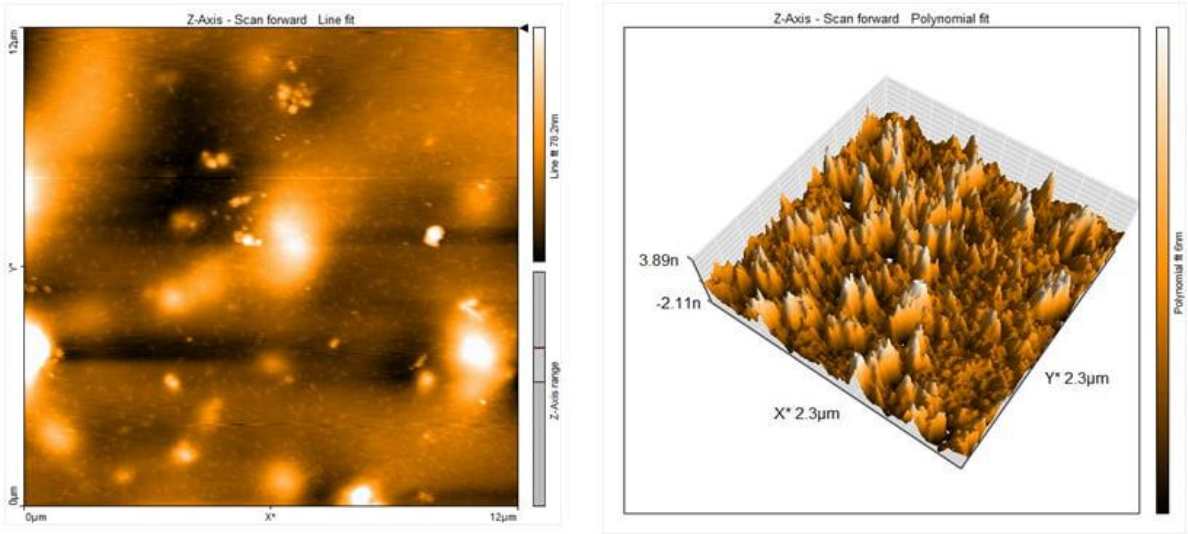

Figure 13. 2D and 3D AFM images of 4 wt% CdS / PVA

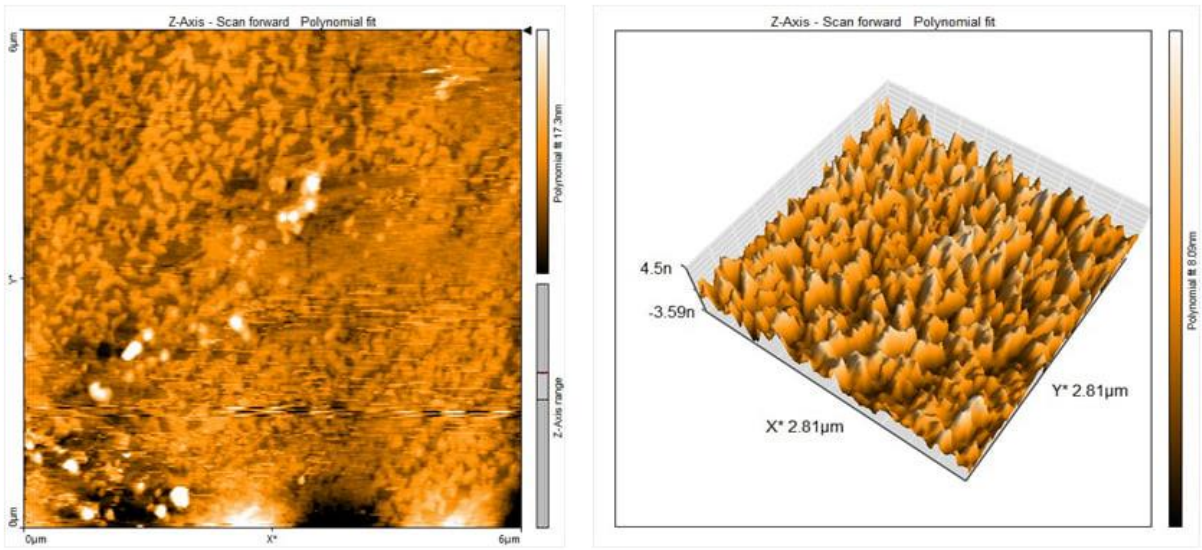

Figure 14. 2D and 3D AFM images of 16 wt% CdS / PVA

Table 4. Display roughness average and grain size (diameter).

Sample	Roughness Average (nm)	Grain Size (nm)
Pure PVA	1.5	18.2
4%ZnS	18.04	27.51
16%ZnS	36.78	54.29
4%CdS	3.473	29.67
16%CdS	4.173	64.12

Through images of an atomic force microscope, the added NPs are agglomerates with a lower content, so with the increase of these particles the roughness increases and the particle size increases. It has also been noted that the NPs are well dispersed within the polyvinyl chloride, which may be a good influence for the homogeneous growth mark as it This is since the strong interfacial interaction of the functional groups within the compound. In general, increasing the roughness leads to better mechanical properties. Demonstrate Table 4 displays roughness average and grain size of specimens. These are consistent with the results of researchers [23, 29, 30].

3.6 SEM results

Figure 15 display the SEM images for (PVA)with different contents of (ZnS), and (CdS) NPs at different magnification power to study nanocomposite morphology. The Micro SEM images demonstrate that paths network formed of NPs inside the (PVA) where charge carriers are allowed to pass through the paths.

The 2D- scanning electron microscopy (2D-SEM) is commonly used to identify phase separations and interfaces in polymer films for the purpose of studying their compatibility with one another.

In subgraph (a) of Figure 15, the SEM micrograph pure PVA exhibits higher porosity in pure state, but when it is mixing with NPs, in general porosity decreases. in subgraphs (b) and (d) of Figure 15 PVA with CdS and ZnS in the lowest percentage of both. SEM tests appear porous coatings, porous coatings allow the passage of gases or liquids through their interconnected network of pores. While this property can be

advantageous in certain applications, it can be detrimental for blocking IR radiation. The presence of pores in a coating can allow IR radiation to penetrate and pass through, reducing the coating's effectiveness in blocking IR.

Figures 15c and 15e PVA with CdS and ZnS in the largest percentage of both. SEM tests appear non-porous coatings, on the other hand, have a solid, continuous structure without any interconnected pores. This solid structure acts as a barrier against IR radiation, minimizing its transmission through the coating. Non-porous coatings are typically more efficient at blocking IR and can provide better protection against unwanted heat transfer or interference during scanning microscope experiments. In general, non-porous, thin film coating would generally be more suitable and effective. Through the SEM images, the surface is uniform, smooth, and homogeneous in terms of molecular distribution. This may be since NPs are characterized by the self-assembly property, and this leads to an appropriate distribution within the polymer, and this is consistent with the results of AFM. These are consistent with the results of researchers [19, 29, 30].

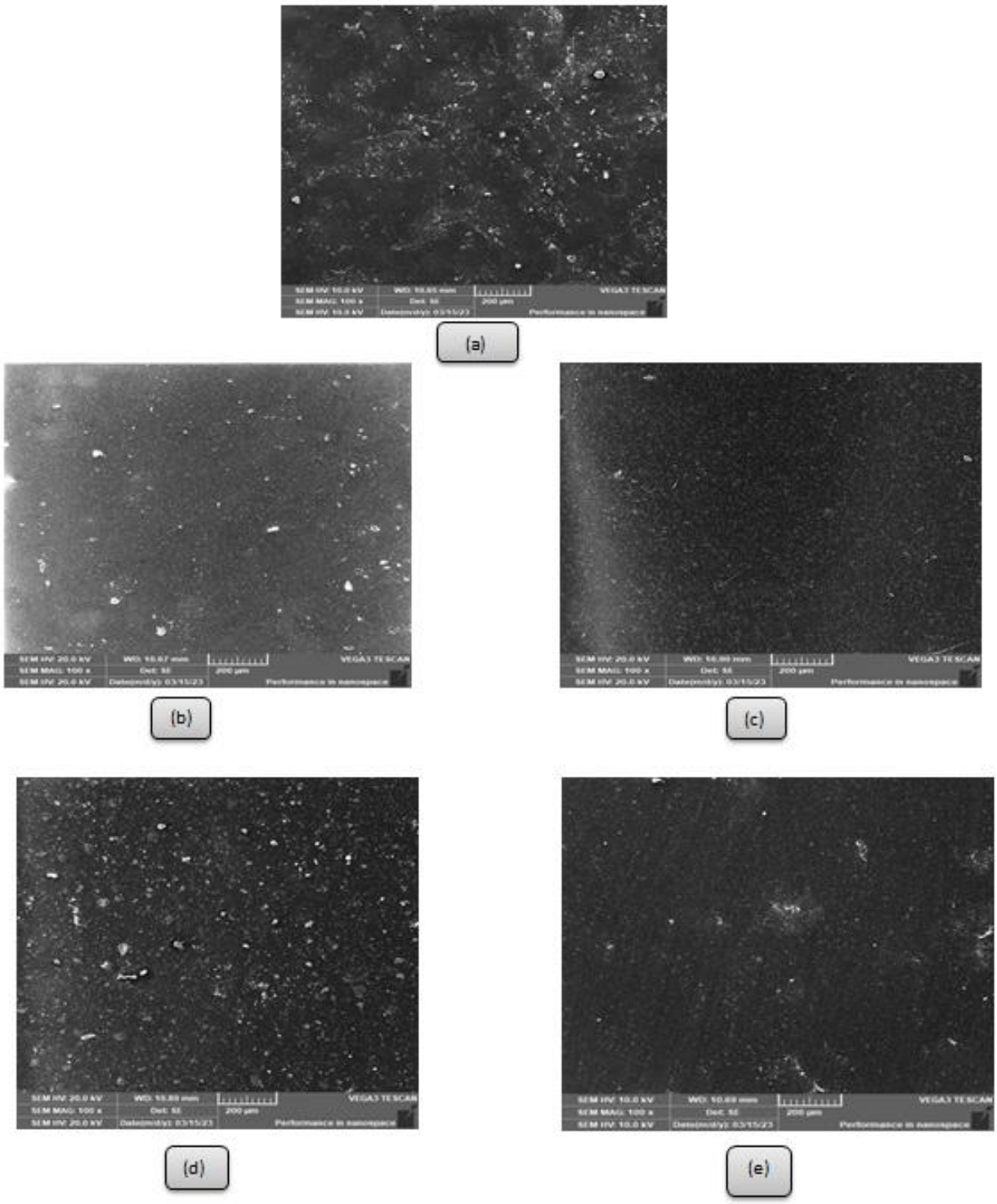

Figure 15. SEM images for a) Pure PVA, b) PVA with 4 wt% ZnS, c) PVA with 16 wt% ZnS, d) PVA with 4 wt% CdS, e) PVA with 16 wt% CdS

4. CONCLUSION

The study explores coatings designed to block infrared (IR) radiation, using polyvinyl alcohol (PVA) mixed with cadmium sulfide (CdS) or zinc sulfide (ZnS) at 4%, 12%, and 16% concentrations. It notice that by increasing the nanoparticle content, the infrared blocking increases. Analytical techniques like DSC, TGA, FTIR, UV-Vis spectroscopy, AFM, and SEM were employed to evaluate their properties. SEM and AFM affirmed uniform dispersion of NPs in the PVA matrix. DSC revealed potential changes in phase transitions and thermal stability due to CdS/ZnS variations. TGA demonstrated improved thermal stability compared to pure PVA, essential for applications with temperature variations. FTIR and UV-Vis spectroscopy unveiled molecular structures and optical traits, indicating CdS/ZnS concentrations' effect on IR-blocking and visible light transmission. AFM and SEM disclosed surface morphology and distribution of CdS/ZnS particles within the matrix. The study underscores the potential of PVA/CdS and PVA/ZnS coatings to manage IR radiation effectively. Utilizing diverse techniques deepened insights into their thermal, optical, and morphological properties. Increased NPs enhanced UV radiation resistance and insulation.ZnS/PVA and PVA/CdS coatings serve critical roles in various real-world applications by effectively blocking or regulating the transmission of infrared (IR) radiation. Their practical significance includes thermal insulation in architecture and automotive sectors, enabling temperature control and reducing the need for excessive heating or cooling. These coatings are also valuable in optical devices, safeguarding lenses, windows, and sensors from IR interference while enhancing their performance. Additionally, they find use in protective coatings for materials sensitive to IR radiation, such as electronic components and artwork. Moreover, these coatings contribute to energy efficiency by managing heat transmission, subsequently reducing energy costs and environmental impact in buildings and vehicles. Their applications span diverse industries, playing a vital role in improving functionality, efficiency, and protection in everyday scenarios. When exploring the efficacy of "Blocking infrared rays by PVA/CdS or PVA/ZnS coating," key suggestions involve optimizing material ratios, assessing coating durability, and exploring multilayer compositions. However, limitations encompass long-term stability and feasibility for large-scale production. To enhance ZnS/CdS performance, nanostructuring, doping, and surface modifications serve as potential strategies for strengthening and improving their overall performance.

REFERENCES

[1] Al-Yasiri, Q., Szabó, M. (2021). Incorporation of phase change materials into building envelope for thermal comfort and energy saving: A comprehensive analysis. Journal of Building Engineering, 36: 102122. https://doi.org/10.1016/j.jobe.2020.102122

[2] Baranwal, N., Mahulikar, S.P. (2019). Review of Infrared signature suppression systems using optical blocking method. Defence Technology, 15(3): 432-439. https://doi.org/10.1016/j.dt.2018.12.002

[3] Kadem, B.Y., Al-Hashimi, M., Hasan, A.S., Kadhim, R.G., Rahaq, Y., Hassan, A.K. (2018). The effects of the PEDOT: PSS acidity on the performance and stability of P3HT: PCBM-based OSCs. Journal of Materials Science: Materials in Electronics, 29: 19287-19295. https://doi.org/10.1007/s10854-018-0055-4

[4] Chai, X., Zhu, D., Liu, Y., Qing, Y., Ren, Z., Luo, F., Li, P. (2021). Silver-modified chromium (III) oxide as multi-band compatible stealth materials for visual/infrared stealth and radar wave transmission. Composites Science and Technology, 216: 109038. https://doi.org/10.1016/j.compscitech.2021.109038

[5] Chen, L., Ren, Z., Liu, X., Wang, K., Wang, Q. (2021). Infrared–visible compatible stealth based on Al-SiO_2 nanoparticle composite film. Optics Communications, 482: 126608. https://doi.org/10.1016/j.optcom.2020.126608

[6] Fan, W., Zhang, X., Zhang, Y., Zhang, Y., Liu, T. (2019). Lightweight, strong, and super-thermal insulating polyimide composite aerogels under high temperature. Composites Science and Technology, 173: 47-52. https://doi.org/10.1016/j.compscitech.2019.01.025

[7] Hasan, A.S., Kadem, B.Y., Akraa, M.A., Hassan, A.K. (2020). PVA: PEDOT: PSS: Carbon based nano-composites for pressure sensor applications. Digest Journal of Nanomaterials and Biostructures, 15(1): 197-205.

[8] Zhang, X., Zhao, X., Xue, T., Yang, F., Fan, W., Liu, T. (2020). Bidirectional anisotropic polyimide/bacterial cellulose aerogels by freeze-drying for super-thermal insulation. Chemical Engineering Journal, 385: 123963. http://doi.org/10.1016/j.cej.2019.123963

[9] Wu, M.Q., Wu, S., Cai, Y.F., Wang, R.Z., Li, T.X. (2021). Form-stable phase change composites: Preparation, performance, and applications for thermal energy conversion, storage and management. Energy Storage Materials, 42: 380-417. https://doi.org/10.1016/j.ensm.2021.07.019

[10] Mohammed, F.Q., Edan, M.S., Hasan, A.S., Haider, A.J. (2021). Synthesis and theoretical concepts of boron nitride nanowires grown on nitrides stainless steel surface by hybrid gas phase process. In Key Engineering Materials, 886: 97-107. https://doi.org/10.4028/www.scientific.net/KEM.886.97

[11] Regmi, A., Basnet, Y., Bhattarai, S., Gautam, S.K. (2023). Cadmium sulfide nanoparticles: Synthesis, characterization, and antimicrobial study. Journal of Nanomaterials, 2023: Article ID 8187000. https://doi.org/10.1155/2023/8187000

[12] Singh, B.R., Dwivedi, S., Al-Khedhairy, A.A., Musarrat, J. (2011). Synthesis of stable cadmium sulfide nanoparticles using surfactin produced by Bacillus amyloliquifaciens strain KSU-109. Colloids and Surfaces B: Biointerfaces, 85(2): 207-213. https://doi.org/10.1016/j.colsurfb.2011.02.030

[13] Salavagione, H.J., Quiles-Díaz, S., Shuttleworth, P.S., Ellis, G.J., Gómez-Fatou, M.A. (2020). Encyclopedia of Polymer Science and Technology Graphene Functionalization for Polymer Nanocomposites.

[14] Alva, G., Lin, Y., Liu, L., Fang, G. (2017). Synthesis, characterization and applications of microencapsulated phase change materials in thermal energy storage: A review. Energy and Buildings, 144: 276-294. http://doi.org/10.1016/j.enbuild.2017.03.063

[15] Habeeb, S.A., Hasan, A.S., Ţălu, Ş., Jawad, A.J. (2021). Enhancing the properties of styrene-butadiene rubber by adding borax particles of different sizes. Iranian Journal

of Chemistry and Chemical Engineering, 40(5): 1616-1629. http://doi.org/10.30492/ijcce.2020.40535

[16] Kuang, T., Jin, M., Lu, X., Liu, T., Vahabi, H., Gu, Z., Gong, X. (2023). Functional carbon dots derived from biomass and plastic wastes. Green Chemistry, 25(17): 6581-6602. https://doi.org/10.1039/D3GC01763J

[17] Abud, S.H., Hasan, A.S., Almaamori, M., Bayan, N. (2021). Enhancement the ability to pump crude oil using rubber solutions. In Journal of Physics: Conference Series, 1818(1): 012235. https://doi.org/10.1088/1742-6596/1818/1/012235

[18] Pattabi, M., Amma, B.S., Manzoor, K., Sanjeev, G. (2007). Effect of 8 MeV electron irradiation on the optical properties of PVP capped CdS nanoparticles in PVA matrix. Solar energy materials and solar cells, 91(15-16): 1403-1407. https://doi.org/10.1016/j.solmat.2007.04.015

[19] Kadhim, M.H., Hasan, A.S., Akraa, M.A., Layla, A.Y. (2021). Preparation and optimization of heterojunction donor (DLC)–acceptor (SI) as a solar cell by DFT and PLD. Journal of Ovonic Research, 2021: 273-281.

[20] Kumar, R.V., Koltypin, Y., Cohen, Y.S., Cohen, Y., Aurbach, D., Palchik, O., Gedanken, A. (2000). Preparation of amorphous magnetite nanoparticles embedded in polyvinyl alcohol using ultrasound radiation. Journal of Materials Chemistry, 10(5): 1125-1129. https://doi.org/10.1039/B000440P

[21] Jebur, S.K., Braihi, A.J., Hassan, A.S. (2022). Graphene effects on the structural, morphological and optical properties of PEDOT: PSS thin films. Materials Today: Proceedings, 49: 2733-2740. http://doi.org/10.1016/j.matpr.2021.09.255

[22] Qian, X.F., Yin, J., Huang, J.C., Yang, Y.F., Guo, X.X., Zhu, Z.K. (2001). The preparation and characterization of PVA/Ag2S nanocomposite. Materials Chemistry and Physics, 68(1-3): 95-97. https://doi.org/10.1016/S0254-0584(00)00288-1

[23] El-Naggar, A.M., Heiba, Z.K., Kamal, A.M., Abd-Elkader, O.H., Mohamed, M.B. (2023). Impact of ZnS/Mn on the structure, optical, and electric properties of PVC polymer. Polymers, 15(9): 2091. https://doi.org/10.3390/polym15092091

[24] Sarma, S., Mothudi, B.M., Dhlamini, M.S. (2016). Observed coexistence of memristive, memcapacitive and meminductive characteristics in polyvinyl alcohol/cadmium sulphide nanocomposites. Journal of Materials Science: Materials in Electronics, 27: 4551-4558. https://doi.org/10.1007/s10854-016-4330-y

[25] Rudenko, E., Tsybrii, Z., Sizov, F., Korotash, I., Polotskiy, D., Skoryk, M., Svezhentsova, K. (2017). Infrared blocking, microwave and terahertz low-loss transmission AlN films grown on flexible polymeric substrates. Journal of Applied Physics, 121(13): 135304. http://doi.org/10.1063/1.4979858

[26] Kargarzadeh, H., Mariano, M., Huang, J., Lin, N., Ahmad, I., Dufresne, A., Thomas, S. (2017). Recent developments on nanocellulose reinforced polymer nanocomposites: A review. Polymer, 132: 368-393. https://doi.org/10.1016/j.polymer.2017.09.043

[27] Sirait, M. (2017). Synthesis and morphology of polyvinyl alcohol/zinc sulfide nanocomposite. In IOP Conference Series: Materials Science and Engineering 223(1): 012027. https://doi.org/10.1088/1757-899X/223/1/012027

[28] Wang, C.F., Cheng, R., Ji, W.Q., Ma, K., Ling, L., Chen, S. (2018). Recognition of latent fingerprints and ink-free printing derived from interfacial segregation of carbon dots. ACS Applied Materials & Interfaces, 10(45): 39205-39213. https://doi.org/10.1021/acsami.8b13545

[29] Rao, G.A., Mahulikar, S.P. (2002). Integrated review of stealth technology and its role in airpower. The Aeronautical Journal, 106(1066): 629-642. http://doi.org/10.1017/S0001924000011702

[30] Pandian, S.R.K., Deepak, V., Kalishwaralal, K., Gurunathan, S. (2011). Biologically synthesized fluorescent CdS NPs encapsulated by PHB. Enzyme and Microbial Technology, 48(4-5): 319-325. http://doi.org/10.1016/j.enzmictec.2011.01.005